SCIENCE CHINA
Information Sciences

• RESEARCH PAPER •

September 2014, Vol. 57 092202:1–092202:12
doi: 10.1007/s11432-013-4965-8

Leader-follower formation control without leader's velocity information

SHEN DongBin[1], SUN ZhenDong[2] & SUN WeiJie[1]*

[1]*College of Automation Science and Engineering, South China University of Technology, Guangzhou* 510640*, China;*
[2]*Key Laboratory of Systems & Control, Academy of Mathematics and Systems Science, Chinese Academy of Sciences, Beijing* 100193*, China*

Received April 5, 2013; accepted June 9, 2013; published online July 16, 2014

Abstract In this paper, we consider the mobile robots formation control problem without direct measurement of the leader robot's linear velocity. Two decentralized nonlinear algorithms are proposed, respectively, based on adaptive dynamic feedback and immersion & invariance estimation based second order sliding mode control methodologies. The main idea is to solve formation problem by estimating the leader robots's linear velocity, while maintaining the given predefined separation distance and bearing angle between the leader robot and the follower robot. The stability of the closed-loop system is proven by means of the Lyapunov method. The proposed controllers are smooth, continuous and robust against unknown bounded uncertainties such as sensor inaccuracy between the outputs of sensors and the true values in collision free environments. Simulation examples and physical vehicles experiments are presented to verify the effectiveness of the proposed design approaches, and the proposed designed methodologies are carefully compared to illustrate the pros and cons of the approaches.

Keywords nonholonomic mobile robots, leader-follower formation, adaptive dynamic feedback, adaptive estimation, immersion & invariance

Citation Shen D B, Sun Z D, Sun W J. Leader-follower formation control without leader's velocity information. Sci China Inf Sci, 2014, 57: 092202(12), doi: 10.1007/s11432-013-4965-8

1 Introduction

Over the last decade, controlling groups of unmanned vehicles has been attracting widespread attention in the literature [1–3]. As a promising technology, the multi-agent distributed formation control has many advantages over conventional centralized control methodologies such as enhancing the robustness and efficiency and providing redundancy and reconfiguration ability [4–6].

Robots formation control is to control several robots to get into some desired shapes and maintain the formations during their moving. These robots are not physically coupled in any way and can communicate with each other through wireless technology. Various formation control laws have been proposed for designing strategies of nonholonomic vehicles [7–10]. One of the most popular methods is the leader-follower based formation control algorithm, where one of the robots is considered as the leader and the others as the followers. The leader robot tracks a predesigned trajectory and the follower robots are required to stay at a specified separation distance and bearing angle from the leader robot [1]. Ref. [5] proposed a

*Corresponding author (email: auwjsun@scut.edu.cn)

formation controller based on the input and output linearization methods and proper transfer function approximation. Ref. [9] controlled the formation variables to a desired manifold via the sliding mode control method. The above references assumed that the states such as position, velocity and orientation are available for controllers. However, when some components of the state cannot be measured directly or the measurement quality is poor, they have to be estimated through some suitable observers [11]. For this, the extended and unscented Kalman filters have been widely used to design observers based on a priori knowledge about noises [12,13], but the complex mathematical deduction restricts their implementations and applications [11]. Using the immersion & invariance method, Ref. [11] presented a vision based range estimator for the follower robot under the assumption that there exist sensor limitations causing unreliable information exchanges between the leader and follower robots. Velocity observers have also been proposed for the consensus problem among multiple agents system without velocity measurements in [14]. The observer for an agent was designed based on its neighbors' coordinates on the global Cartesian plane. Thus, all of the robots should be embedded into a positioning device in practice such as GPS device. This is inconvenient or impossible in some poor environments, for example, when there is not any GPS signal.

To tackle this dilemma, this paper focuses on controller design for nonholonomic mobile robots in leader-follower formation form where the leader robot's linear velocity is not available. We assume that the leader robot's linear velocity is constant, which has its actual technical sense. When the leader has a constant linear velocity and a dynamic angular velocity, the robots in fact can track any sufficiently continuous trajectory in theory since the radius of the trajectory is equal to the ratio of the linear velocity over the angular velocity. The problem has been solved based upon the methodologies of adaptive dynamic feedback [15] and invariant manifold approach [16], independently. In the latter approach, as in [15,16], the adaptive controller is first designed as a parameter update law. To provide smooth control signals and attenuate the chattering phenomenon, a second-order sliding mode algorithm is further provided to derive the control methodology for the follower robots [7,8]. Under the proposed methods, the follower robots are manipulated to get into and maintain the formation in the sense that each follower can track the leader robot in a preassigned separation distance and bearing angle without knowing the leader robot's linear velocity and only using the local information between the leader and follower robots. Notice that a similar scheme has been presented in [17]; however, the theoretical development there is problematic. In fact, as both $e_2(t)$ and α are functions of sign-indefinite and they are not correlated in any way, the inequality (10) in [17] in general would not hold true nor can make an absolute value of a time variant function not larger than $-e_2(t)\alpha$ over a positive function. Therefore, the proof of the main theoretical result Theorem 1 is incorrect.

The main contribution of this work lies in the following aspects. On the one hand, the formation control problem is investigated without knowing the leader robot's linear velocity. The immersion & invariance based estimation approach is first proposed to estimate the leader robot's linear velocity and formation state variables then a second order sliding mode control algorithm is further chosen to design formation controllers. On the other hand, the proposed controller design methodologies only use local state variables to construct estimators. In a poor environment, it is much easier to get relative position information rather than global information compared with global state observer design.

The rest of the paper is organized as follows. In Section 2, we introduce the model of leader-follower based formation of two mobile robots. Section 3 develops the nonlinear adaptive dynamic feedback control law. Section 4 presents the immersion & invariance estimation based approach for the leader robot's linear velocity and formation variables, based on which a second order sliding mode control law is further designed. The numeric simulations and experiments are given in Section 5 and Section 6, respectively. Finally, conclusion is made in Section 7.

2 Dynamic model of nonholonomic mobile robots

Consider a team of velocity-controlled nonholonomic robots which are interacting with each other or with the environment. The objective is to control the robots to form a desired formation. The coordinates of

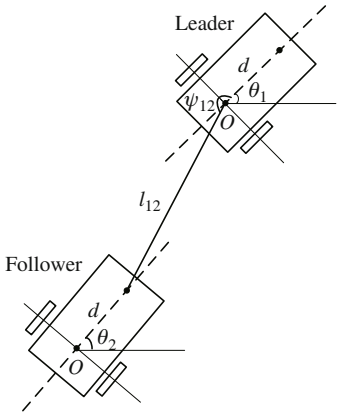

Figure 1 $l-\psi$ based formation control.

the ith vehicle's position in the Cartesian plane is denoted by (x_i, y_i) and the orientation with respect to the inertial reference frame is denoted by θ_i. Let the linear velocity and angular velocity of the mobile robot be v_i and ω_i, respectively. Then the kinematic equations of the system are expressed as

$$\dot{x}_i = v_i \cos\theta_i, \quad \dot{y}_i = v_i \sin\theta_i, \quad \dot{\theta}_i = \omega_i.$$

Consider a formation of two mobile robots moving on a plane, as shown in Figure 1, where each robot is actuated by two driving rear wheels mounted on the same axis. The robot acting as the leader is numbered as robot 1 while the other robot as the follower is numbered as robot 2. The distance l_{12} between the two robots is denoted from the center of the leader robot's two rear wheels to the front of the follower robot (offset by d from the center of the follower robot's two rear wheels). And the bearing angle ψ_{12} is measured from the line of orientation of the leader to the distance line between the two robots. In order to avoid collisions, we suppose that l_{12} is large enough. The task here is to design a controller to force the follower robot to track the leader robot with some predesigned separation distance l_{12} and bearing angle ψ_{12} when they move.

In order to form the formation, the follower robot should also satisfy the following formation equation set [5]:

$$\begin{aligned} \dot{l}_{12} &= v_2 \cos\gamma_1 - v_1 \cos\psi_{12} + d\omega_2 \sin\gamma_1, \\ \dot{\psi}_{12} &= \frac{1}{l_{12}}\{v_1 \sin\psi_{12} - v_2 \sin\gamma_1 + d\omega_2 \cos\gamma_1 - l_{12}\omega_1\}, \\ \dot{\theta}_2 &= \omega_2, \end{aligned} \tag{1}$$

where $\gamma_1 = \theta_1 + \psi_{12} - \theta_2$.

3 Adaptive control as dynamic feedback

In this section, we use the adaptive dynamic feedback control method [15] to study the formation problem. The linear velocity v_1 of the leader robot is supposed to be constant and cannot be measured directly. Firstly, an estimator is proposed to estimate the unavailable leader robot's linear velocity and then the control law is derived.

Choose the input of (1) as $\boldsymbol{u}_2 = [v_2, \omega_2]^{\mathrm{T}}$ and denote $\theta_e = \theta_2 - \theta_1$. System (1) can be re-written as

$$\begin{bmatrix} \dot{l}_{12} \\ \dot{\psi}_{12} \end{bmatrix} = \boldsymbol{G}_a \boldsymbol{u}_2 + \boldsymbol{f}_a + v_1 \boldsymbol{\varphi}, \tag{2}$$

$$\dot{\theta}_e = \omega_2 - \omega_1, \tag{3}$$

where

$$\boldsymbol{f}_a = \begin{bmatrix} 0 \\ -\omega_1 \end{bmatrix}, \ \boldsymbol{G}_a(l_{12}, \psi_{12}, \gamma_1) = \begin{bmatrix} \cos\gamma_1 & d\sin\gamma_1 \\ -\frac{\sin\gamma_1}{l_{12}} & \frac{d\cos\gamma_1}{l_{12}} \end{bmatrix}, \ \boldsymbol{\varphi}(l_{12}, \psi_{12}) = \begin{bmatrix} -\cos\psi_{12} \\ \frac{\sin\psi_{12}}{l_{12}} \end{bmatrix}.$$

Since $\det(\boldsymbol{G}_a) = d/l_{12} \neq 0$, the inverse of $\boldsymbol{G}_a$ exists.

Denote the desired separation distance and bearing angle by l_{d12} and ψ_{d12} which can be some constant values. Then we can obtain the tracking error $\boldsymbol{e}_a = [l_{12} - l_{d12}, \psi_{12} - \psi_{d12}]^{\mathrm{T}} = [l_{e12}, \psi_{e12}]^{\mathrm{T}}$.

The estimator for the unmeasured linear velocity of the leader robot v_1 is given by

$$\dot{\widehat{v}}_1 = \kappa \boldsymbol{e}_a^{\mathrm{T}} \boldsymbol{\varphi}, \tag{4}$$

where κ is the adaptation gain. The dynamics of the estimate error $\widetilde{v}_1 = \widehat{v}_1 - v_1$ is expressed as

$$\dot{\widetilde{v}}_1 = \kappa \boldsymbol{e}_a^{\mathrm{T}} \boldsymbol{\varphi}. \tag{5}$$

Theorem 1. The tracking error $\boldsymbol{e}_a$ asymptotically converges to zero if the follower robot is with the control law $\boldsymbol{u}_2 = \boldsymbol{G}_a^{-1}(-k\boldsymbol{e}_a - \boldsymbol{f}_a - \widehat{v}_1\boldsymbol{\varphi})$, where $k > 0$ is a constant gain. And θ_e is bounded under the condition that $v_1 \geqslant V_{1\min}$, $|\omega_1| < W_{\max}$, and $|\theta_e(0)| < \Theta$ for some positive constants $V_{1\min}$, $W_{\max}$, and Θ.

Proof. Substituting $\boldsymbol{u}_2$ into (2), we can obtain

$$\dot{\boldsymbol{e}}_a = -k\boldsymbol{e}_a - \widetilde{v}_1\boldsymbol{\varphi}. \tag{6}$$

Choose a Lyapunov function $V_1(\boldsymbol{e}_a, \widetilde{v}_1) = \frac{1}{2}\boldsymbol{e}_a^{\mathrm{T}}\boldsymbol{e}_a + \frac{1}{2\kappa}\widetilde{v}_1^2$. The derivative of V_1 can be calculated as

$$\dot{V}_1 = \boldsymbol{e}_a^{\mathrm{T}}\dot{\boldsymbol{e}}_a + \frac{1}{\kappa}\widetilde{v}_1\dot{\widetilde{v}}_1 = -k\boldsymbol{e}_a^{\mathrm{T}}\boldsymbol{e}_a - \widetilde{v}_1\left(\boldsymbol{e}_a^{\mathrm{T}}\boldsymbol{\varphi} - \frac{1}{\kappa}\dot{\widetilde{v}}_1\right) = -k\boldsymbol{e}_a^{\mathrm{T}}\boldsymbol{e}_a \leqslant 0.$$

As a result, the equilibrium $\Omega = \{(\boldsymbol{e}_a, \widetilde{v}_1) | \boldsymbol{e}_a = \boldsymbol{0},\ \widetilde{v}_1 = 0\}$ of (5) and (6) is stable. Let $\dot{V}_1 = 0$. Then we have $\boldsymbol{e}_a = \boldsymbol{0}$. Substituting $\boldsymbol{e}_a = \boldsymbol{0}$ into (6) yields $\widetilde{v}_1\boldsymbol{\varphi} = \widetilde{v}_1[-\cos\psi_{12}, \sin\psi_{12}/l_{12}]^{\mathrm{T}} = \boldsymbol{0}$. Since l_{12} is bounded and it is known that $\sin\psi_{12}$ and $\cos\psi_{12}$ are not equal to zero simultaneously, it can be concluded that $\widetilde{v}_1 = 0$. Thus, the largest invariant set for systems (5) and (6) is $\Omega = \{\boldsymbol{e}_a = \boldsymbol{0},\ \widetilde{v}_1 = 0\}$. By LaSalle's invariance principle, we have $\lim_{t\to\infty}\boldsymbol{e}_a = \boldsymbol{0}$ and $\lim_{t\to\infty}\widetilde{v}_1 = 0$.

Next, we show that $\theta_e(t)$ is always bounded when $v_1 \geqslant V_{1\min}$ and $|\omega_1| < W_{\max}$. Applying the following coordinate transformation: $\zeta_1 = l_{e12},\ \zeta_2 = \psi_{e12},\ \zeta_3 = \theta_e$, we obtain the zero dynamics of systems (2) and (3) in the new coordinate as

$$\dot{\zeta}_3 = -\frac{v_1}{d}\sin\zeta_3 + \frac{l_{d12}}{d}\omega_1\cos(\psi_{d12} - \zeta_3) - \omega_1. \tag{7}$$

The nominal system for (7) is

$$\dot{\zeta}_3 = -\frac{v_1}{d}\sin\zeta_3. \tag{8}$$

Choosing a Lyapunov function $V_2(\zeta_3) = \frac{1}{2}\zeta_3^2$ for the system leads to

$$\dot{V}_2(\zeta_3) = \zeta_3\dot{\zeta}_3 = -\frac{v_1}{d}\zeta_3\sin\zeta_3 \leqslant -\frac{V_{1\min}}{d}\sin^2\zeta_3, \tag{9}$$

where $\zeta_3 \in (-\pi/2, \pi/2)$. Accordingly, $\zeta_3 = 0$ is a locally asymptotically stable equilibrium of the nominal system (8). Furthermore, it is known that $V_2(\zeta_3)$ satisfies the following inequations:

$$\alpha_1(\|\zeta_3\|) \leqslant V_2(\zeta_3) \leqslant \alpha_2(\|\zeta_3\|),\quad \frac{\partial V_2}{\partial\zeta_3}\dot{\zeta}_3 \leqslant -\alpha_3(\|\zeta_3\|),\quad \left\|\frac{\partial V_2}{\partial\zeta_3}\right\| \leqslant \alpha_4(\|\zeta_3\|),$$

where $\alpha_1(\|\zeta_3\|) = \alpha_2(\|\zeta_3\|) = \frac{1}{2}\|\zeta_3\|^2,\ \alpha_3(\|\zeta_3\|) = \frac{V_{1\min}}{d}\sin^2(\|\zeta_3\|), \alpha_4(\|\zeta_3\|) = \|\zeta_3\|$. Choose the positive constants μ and Θ where $\mu \in (0,1)$ and $\Theta \in (0, \pi/2)$. And define the interval $D = \{\zeta_3 \in R | \|\zeta_3\| < \Theta\}$. Denote $\|g(\zeta_3)\| = \|\frac{l_{d12}}{d}\omega_1\cos(\psi_{d12} - \zeta_3) - \omega_1\| = \iota$ and let $\iota < \mu\alpha_3(\alpha_2^{-1}(\alpha_1(\Theta)))/\alpha_4(\Theta)$. Then we can obtain $\|\omega_1\| < \frac{\mu V_{1\min}\sin^2\Theta}{(l_{d12}+d)\Theta} = W_{\max}$. If the initial condition $\zeta_3(0)$ satisfies $\|\zeta_3(0)\| < \alpha_2^{-1}(\alpha_1(\Theta)) = \Theta$, then

$$\begin{cases} \|\zeta_3(t)\| \leqslant \beta(\|\zeta_3(0)\|, t), & \forall\ 0 \leqslant t < T, \\ \|\zeta_3(t)\| \leqslant \hbar(\iota), & t \geqslant T, \end{cases}$$

for some finite time T, where β is a $\mathcal{KL}$ function and

$$\hbar(\iota) = \alpha_1^{-1}\left(\alpha_2\left(\alpha_3^{-1}\left(\frac{\iota\alpha_4(\Theta)}{\mu}\right)\right)\right) < \Theta,$$

which implies that $\theta_e(t) \in (-\Theta, \Theta)$.

4 Immersion & invariance estimation based second order sliding mode control

The controllers proposed in the previous section provide a way to form a formation without direct measurement of the leader robot's linear velocity. Since this algorithm does not consider any disturbances in the system, the performance of controllers largely depends on the accuracy of the system's model and is vulnerable to uncertainties. To overcome this defect, we construct an immersion & invariance estimation based second order sliding mode controller in this section .

4.1 Immersion & invariance based estimator design methodology

Consider a type of nonlinear systems

$$\dot{\boldsymbol{x}} = \boldsymbol{f}_1(\boldsymbol{x}, \boldsymbol{u}) + \boldsymbol{\Phi}(\boldsymbol{x})\boldsymbol{\vartheta}, \tag{10}$$

where $\boldsymbol{x} \in \mathbb{R}^n$ is the state vector and $\boldsymbol{u} \in \mathbb{R}^m$ is the input, $\boldsymbol{f}_1(\boldsymbol{x}, \boldsymbol{u}) = [f_1(\boldsymbol{x}, \boldsymbol{u}), \ldots, f_n(\boldsymbol{x}, \boldsymbol{u})]^{\mathrm{T}}$ and $\boldsymbol{\Phi}(\boldsymbol{x}) \in \mathbb{R}^{n\times p}$ are known smooth matrices, and $\boldsymbol{\vartheta} \in \mathbb{R}^p$ with $p \geqslant n$ is an unknown constant parameter vector. Furthermore, $\boldsymbol{\Phi}(\boldsymbol{x})\boldsymbol{\vartheta}$ has the form $\boldsymbol{\Phi}(\boldsymbol{x})\boldsymbol{\vartheta} = [\boldsymbol{\vartheta}_1^{\mathrm{T}}\boldsymbol{\varphi}_1(\boldsymbol{x}), \ldots, \boldsymbol{\vartheta}_n^{\mathrm{T}}\boldsymbol{\varphi}_n(\boldsymbol{x})]^{\mathrm{T}}$ with $\boldsymbol{\vartheta}_i \in \mathbb{R}^{p_i}$, $\boldsymbol{\varphi}_i \in \mathbb{R}^{p_i}$ and $\sum_{i=1}^n p_i = p$. The objective is to derive an estimator for $\boldsymbol{\vartheta}$ and present an asymptotic estimator $\widehat{\boldsymbol{x}}$ for $\boldsymbol{x}$.

Construct state observers

$$\dot{\widehat{x}}_i = f_i(\boldsymbol{x}, \boldsymbol{u}) + \boldsymbol{\varphi}_i^{\mathrm{T}}(\boldsymbol{x})\widehat{\boldsymbol{\vartheta}}_i - k_i(\boldsymbol{x}, \boldsymbol{r}, \widehat{\boldsymbol{x}} - \boldsymbol{x})(\widehat{x}_i - x_i) \tag{11}$$

for $i = 1, \ldots, n$. Let $\boldsymbol{z} = [\boldsymbol{z}_1^{\mathrm{T}}, \ldots, \boldsymbol{z}_n^{\mathrm{T}}]^{\mathrm{T}}$ and $\boldsymbol{r} = [r_1, \ldots, r_n]^{\mathrm{T}}$ with

$$\boldsymbol{z}_i = \frac{\widehat{\boldsymbol{\vartheta}}_i - \boldsymbol{\vartheta}_i}{r_i} = \frac{\boldsymbol{\xi}_i + \boldsymbol{\beta}_i(x_i, \widehat{\boldsymbol{x}}) - \boldsymbol{\vartheta}_i}{r_i}, \tag{12}$$

where $\boldsymbol{\xi}_i$ denote the estimator states, r_i are scaling factors, and $k_i(\cdot)$ and $\boldsymbol{\beta}_i(x_i, \widehat{\boldsymbol{x}})$ are functions to be specified for $\widehat{\boldsymbol{x}} = [\widehat{x}_1, \ldots, \widehat{x}_n]^{\mathrm{T}}$. The update laws of $\boldsymbol{\xi}_i$ are designed as

$$\dot{\boldsymbol{\xi}}_i = -\frac{\partial\boldsymbol{\beta}_i}{\partial x_i}\left(f_i(\boldsymbol{x}, \boldsymbol{u}) + \boldsymbol{\varphi}_i^{\mathrm{T}}(\boldsymbol{x})\widehat{\boldsymbol{\vartheta}}_i\right) - \sum_{j=1}^n \frac{\partial\boldsymbol{\beta}_i}{\partial\widehat{x}_j}\dot{\widehat{x}}_j, \tag{13}$$

which yields the derivative of (12)

$$\dot{\boldsymbol{z}}_i = -\frac{\partial\boldsymbol{\beta}_i}{\partial x_i}\boldsymbol{\varphi}_i^{\mathrm{T}}(\boldsymbol{x})\boldsymbol{z}_i - \frac{\dot{r}_i}{r_i}\boldsymbol{z}_i. \tag{14}$$

Choose the update laws for $\boldsymbol{\beta}_i(x_i, \widehat{x})$ in (14) as

$$\boldsymbol{\beta}_i(x_i, \widehat{x}) = \kappa_i\int_0^{x_i}\boldsymbol{\varphi}_i(\widehat{x}_1, \ldots, \widehat{x}_{i-1}, \tau, \widehat{x}_{i+1}, \ldots, \widehat{x}_n)\mathrm{d}\tau = \kappa_i\int_0^{x_i}\left[\boldsymbol{\varphi}_i(\boldsymbol{x}) - \sum_{j=1}^n e_j\boldsymbol{\delta}_{ij}(\boldsymbol{x}, \boldsymbol{e})\right]\mathrm{d}\tau \tag{15}$$

for some functions $\boldsymbol{\delta}_{ij}(\boldsymbol{x}, \boldsymbol{e})$ with $\boldsymbol{\delta}_{ii}(\boldsymbol{x}, \boldsymbol{e}) = \boldsymbol{0}$, where κ_i, $i = 1, \ldots, n$, are positive constants and $\boldsymbol{e} = [e_1, \ldots, e_n]^{\mathrm{T}}$ with $e_i = \widehat{x}_i - x_i$. Now (14) is transformed into

$$\dot{\boldsymbol{z}}_i = -\kappa_i\boldsymbol{\varphi}_i(\boldsymbol{x})\boldsymbol{\varphi}_i^{\mathrm{T}}(\boldsymbol{x})\boldsymbol{z}_i + \kappa_i\sum_{j=1}^n e_j\boldsymbol{\delta}_{ij}(\boldsymbol{x}, \boldsymbol{e})\boldsymbol{\varphi}_i^{\mathrm{T}}(\boldsymbol{x})\boldsymbol{z}_i - \frac{\dot{r}_i}{r_i}\boldsymbol{z}_i. \tag{16}$$

Then the dynamics of e_i becomes

$$\dot{e}_i = -k_i(\boldsymbol{x}, \boldsymbol{r}, \boldsymbol{e})e_i + r_i\boldsymbol{\varphi}_i^{\mathrm{T}}(\boldsymbol{x})\boldsymbol{z}_i. \tag{17}$$

Choose parameter adjustment laws for r_i and the gain functions k_i in the above equation as

$$\dot{r}_i = c_i r_i \sum_{j=1}^{n} e_j^2 |\boldsymbol{\delta}_{ij}(\boldsymbol{x}, \boldsymbol{e})|^2, \quad r_i(0) = 1, \tag{18}$$

$$k_i(\boldsymbol{x}, \boldsymbol{r}, \boldsymbol{e}) = \lambda_{ai} r_i^2 + \epsilon \sum_{j=1}^{n} c_j r_j^2 |\boldsymbol{\delta}_{ji}(\boldsymbol{x}, \boldsymbol{e})|^2 \tag{19}$$

for $i = 1, \ldots, n$, where $c_i \geqslant \frac{n}{2}\kappa_i$, $\lambda_{ai} > 0$ and $\epsilon > 0$ are constants.

Lemma 1 ([16])**.** Under condition (19), the system composed of (16)–(18) has a globally bounded stable manifold of equilibrium defined by $\Omega = \{(\boldsymbol{z}, \boldsymbol{r}, \boldsymbol{e}) | \boldsymbol{z} = \boldsymbol{e} = \boldsymbol{0}\}$. And $\{\boldsymbol{z}_i(t),\ r_i(t)\} \in \mathcal{L}_\infty,\ e_i(t) \in \mathcal{L}_\infty \cap \mathcal{L}_2$, and $\boldsymbol{\varphi}_i^{\mathrm{T}}(\boldsymbol{x}(t))\boldsymbol{z}_i(t) \in \mathcal{L}_2$, $\forall i \in \{1, \ldots, n\}$. Furthermore, $\boldsymbol{\varphi}_i^{\mathrm{T}}(\boldsymbol{x}(t))\boldsymbol{z}_i(t)$ converges to zero when $\boldsymbol{\varphi}_i(\boldsymbol{x}(t))$ and its time derivative is bounded.

4.2 Immersion & invariance based estimator design for formation system

In this part, by applying the immersion & invariance based method introduced in the previous subsection to design nonlinear observers, we estimate the leader robot's linear velocity and formation tracking variables.

Rewriting system (1) in the form of (10), we obtain

$$\begin{aligned} &f_1(l_{12}, \psi_{12}) = v_2 \cos\gamma_1 + d\omega_2 \sin\gamma_1, \quad f_2(l_{12}, \psi_{12}) = \left(-v_2 \sin\gamma_1 + d\omega_2 \cos\gamma_1 - l_{12}\omega_1\right)/l_{12}, \\ &\boldsymbol{\varphi}_1(l_{12}, \psi_{12}) = -\cos\psi_{12}, \quad \boldsymbol{\varphi}_2(l_{12}, \psi_{12}) = \sin\psi_{12}/l_{12}, \quad \boldsymbol{\vartheta} = [\boldsymbol{\vartheta}_1^{\mathrm{T}}, \boldsymbol{\vartheta}_2^{\mathrm{T}}]^{\mathrm{T}} = [v_1, v_1]^{\mathrm{T}}. \end{aligned}$$

Let $e_1 = \widehat{l}_{12} - l_{12}$ and $e_2 = \widehat{\psi}_{12} - \psi_{12}$ denote observe errors of the formation variable. Referring to (11) and (12), we set the observers and estimators respectively to be

$$\begin{aligned} &\dot{\widehat{l}}_{12} = v_2 \cos\gamma_1 + d\omega_2 \sin\gamma_1 - \widehat{v}_1 \cos\psi_{12} - k_1(\widehat{l}_{12} - l_{12}), \\ &\dot{\widehat{\psi}}_{12} = \frac{1}{l_{12}}\{-v_2 \sin\gamma_1 + d\omega_2 \cos\gamma_1 - l_{12}\omega_1\} + \frac{\sin\psi_{12}}{l_{12}}\widehat{v}_2 - k_2\Big(\widehat{\psi}_{12} - \psi_{12}\Big), \end{aligned} \tag{20}$$

$$\boldsymbol{z}_1 = \frac{\widehat{v}_1 - v_1}{r_1} = \frac{\boldsymbol{\xi}_1 + \boldsymbol{\beta}_1(l_{12}, \widehat{l}_{12}, \widehat{\psi}_{12}) - v_1}{r_1}, \tag{21}$$

$$\boldsymbol{z}_2 = \frac{\widehat{v}_2 - v_1}{r_2} = \frac{\boldsymbol{\xi}_2 + \boldsymbol{\beta}_2(\psi_{12}, \widehat{l}_{12}, \widehat{\psi}_{12}) - v_1}{r_2}. \tag{22}$$

Following (14), denote the update laws for $\boldsymbol{\xi}_1$ and $\boldsymbol{\xi}_2$ by

$$\dot{\boldsymbol{\xi}}_1 = -\frac{\partial \boldsymbol{\beta}_1}{\partial l_{12}}\left(f_1(l_{12}, \psi_{12}) - \widehat{v}_1 \cos\psi_{12}\right) - \frac{\partial \boldsymbol{\beta}_1}{\partial \widehat{l}_{12}}\dot{\widehat{l}}_{12} - \frac{\partial \boldsymbol{\beta}_1}{\partial \widehat{\psi}_{12}}\dot{\widehat{\psi}}_{12}, \tag{23}$$

$$\dot{\boldsymbol{\xi}}_2 = -\frac{\partial \boldsymbol{\beta}_2}{\partial \psi_{12}}\left(f_2(l_{12}, \psi_{12}) + \widehat{v}_2 \frac{\sin\psi_{12}}{l_{12}}\right) - \frac{\partial \boldsymbol{\beta}_2}{\partial \widehat{l}_{12}}\dot{\widehat{l}}_{12} - \frac{\partial \boldsymbol{\beta}_2}{\partial \widehat{\psi}_{12}}\dot{\widehat{\psi}}_{12}. \tag{24}$$

Then the dynamics of (21) and (22) become

$$\dot{\boldsymbol{z}}_1 = -\frac{\partial \boldsymbol{\beta}_1}{\partial l_{12}}(-\cos\psi_{12})\boldsymbol{z}_1 - \frac{\dot{r}_1}{r_1}\boldsymbol{z}_1, \tag{25}$$

$$\dot{\boldsymbol{z}}_2 = -\frac{\partial \boldsymbol{\beta}_2}{\partial \psi_{12}}\left(\frac{\sin\psi_{12}}{l_{12}}\right)\boldsymbol{z}_2 - \frac{\dot{r}_2}{r_2}\boldsymbol{z}_2, \tag{26}$$

where functions $\boldsymbol{\beta}_1,\ \boldsymbol{\beta}_2$ and $\boldsymbol{\varphi}_1(l_{12},\widehat{\psi}_{12}),\ \boldsymbol{\varphi}_2(\widehat{l}_{12},\psi_{12})$ are

$$\begin{aligned}
&\boldsymbol{\beta}_1=\kappa_1\int_0^{l_{12}}(-\cos\widehat{\psi}_{12})\mathrm{d}\tau=-\kappa_1 l_{12}\cos\widehat{\psi}_{12},\quad \boldsymbol{\beta}_2=\kappa_2\int_0^{\psi_{12}}\frac{\sin\tau}{\widehat{l}_{12}}\mathrm{d}\tau=-\kappa_2\frac{\cos\psi_{12}-1}{\widehat{l}_{12}},\\
&\boldsymbol{\varphi}_1(l_{12},\widehat{\psi}_{12})=-\cos\widehat{\psi}_{12}=-\cos\psi_{12}-\frac{\cos(\psi_{12}+e_2)-\cos\psi_{12}}{e_2}e_2=\boldsymbol{\varphi}_1(l_{12},\psi_{12})-e_2\boldsymbol{\delta}_{12},\\
&\boldsymbol{\varphi}_2(\widehat{l}_{12},\psi_{12})=\frac{\sin\psi_{12}}{\widehat{l}_{12}}=\frac{\sin\psi_{12}}{l_{12}}-\frac{\sin\psi_{12}}{l_{12}(l_{12}+e_1)}e_1=\boldsymbol{\varphi}_2(l_{12},\psi_{12})-e_1\boldsymbol{\delta}_{21}.
\end{aligned}$$

Simple calculation gives

$$\dot{\boldsymbol{z}}_1=-\kappa_1\boldsymbol{z}_1\cos^2\psi_{12}-\kappa_1 e_2\boldsymbol{\delta}_{12}\cos\psi_{12}\boldsymbol{z}_1-\frac{\dot{r}_1}{r_1}\boldsymbol{z}_1,\quad \dot{\boldsymbol{z}}_2=-\kappa_2\boldsymbol{z}_2\frac{\sin^2\psi_{12}}{l_{12}^2}+\kappa_2 e_1\boldsymbol{\delta}_{21}\frac{\sin\psi_{12}}{l_{12}}\boldsymbol{z}_2-\frac{\dot{r}_2}{r_2}\boldsymbol{z}_2.$$

And

$$\dot{e}_1=-k_1e_1+r_1\boldsymbol{\varphi}_1^{\mathrm{T}}(l_{12},\psi_{12})\boldsymbol{z}_1,\quad \dot{e}_2=-k_2e_2+r_2\boldsymbol{\varphi}_2^{\mathrm{T}}(l_{12},\psi_{12})\boldsymbol{z}_2,$$

where

$$\begin{aligned}
&k_1=\lambda_{a1}r_1^2+\epsilon c_2r_2^2|\boldsymbol{\delta}_{21}|^2,\quad k_2=\lambda_{a2}r_2^2+\epsilon c_1r_1^2|\boldsymbol{\delta}_{12}|^2,\\
&\dot{r}_1=c_1r_1e_2^2|\boldsymbol{\delta}_{12}|^2,\quad r_1(0)=1,\quad \dot{r}_2=c_2r_2e_1^2|\boldsymbol{\delta}_{21}|^2,\quad r_2(0)=1.
\end{aligned}$$

4.3 Second order sliding formation control

Denote the differences between the observed formation variables and their desired values by $\widehat{l}_{e12}=\widehat{l}_{12}-l_{d12}$ and $\widehat{\psi}_{e12}=\widehat{\psi}_{12}-\psi_{d12}$. Then we have

$$\begin{aligned}
&\dot{\widehat{l}}_{e12}=v_2\cos\gamma_1+d\omega_2\sin\gamma_1-\widehat{v}_1\cos\psi_{12}-k_1\Big(\widehat{l}_{12}-l_{12}\Big),\\
&\dot{\widehat{\psi}}_{e12}=\frac{1}{l_{12}}\{-v_2\sin\gamma_1+d\omega_2\cos\gamma_1-l_{12}\omega_1\}+\frac{\sin\psi_{12}}{l_{12}}\widehat{v}_2-k_2\Big(\widehat{\psi}_{12}-\psi_{12}\Big),\\
&\dot{\theta}_e=\omega_2-\omega_1.
\end{aligned}\tag{27}$$

Define

$$\boldsymbol{f}_2=\begin{bmatrix}-\widehat{v}_1\cos\psi_{12}-k_1(\widehat{l}_{12}-l_{12})\\ \frac{\widehat{v}_2\sin\psi_{12}}{l_{12}}-\omega_1-k_2(\widehat{\psi}_{12}-\psi_{12})\end{bmatrix},\ \boldsymbol{G}=\begin{bmatrix}\cos\gamma_1 & d\sin\gamma_1\\ -\frac{\sin\gamma_1}{l_{12}} & \frac{d\cos\gamma_1}{l_{12}}\end{bmatrix}.$$

Thus the inverse of $\boldsymbol{G}$ exists since $\det(\boldsymbol{G})=d/l_{12}\neq 0$.

Choose the input of system (27) as $\boldsymbol{u}_2=[v_2,\omega_2]^{\mathrm{T}}$ and the output as $\widehat{\boldsymbol{e}}_1=[\widehat{l}_{e12},\widehat{\psi}_{e12}]^{\mathrm{T}}$. The aim now is to design a control input $\boldsymbol{u}_2$ to make $\widehat{\boldsymbol{e}}_1$ converge to zero and obtain a bounded θ_e. For this purpose, consider the following system:

$$\begin{aligned}
&\dot{x}=u,\\
&u=u_1-\lambda|x-f(t)|^{1/2}\mathrm{sgn}(x-f(t)),\\
&\dot{u}_1=-a\mathrm{sgn}(x-f(t)).
\end{aligned}\tag{28}$$

Define a function $\Phi(a,\lambda,C)=|\Psi(t_*)|$, where $(\Sigma(t),\Psi(t))$ is the solution of

$$\begin{aligned}
&\dot{\Sigma}=-|\Sigma|^{1/2}+\Psi,\\
&\dot{\Psi}=\begin{cases}-\frac{1}{\lambda^2}(a-C), & \text{if } -|\Sigma|^{1/2}+\Psi>0,\\ -\frac{1}{\lambda^2}(a+C), & \text{otherwise}\end{cases}
\end{aligned}\tag{29}$$

with $\Sigma(0)=0,\ \Psi(0)=1,\ a>C,\ \lambda\neq 0$, and $t_*=\inf\{t|t>0,\Sigma(t)=0,\Psi(t)<0\}$.

Lemma 2 ([7])**.** Suppose that $a>C>0,\ \lambda>0$, and $\Phi(a,\lambda,C)<1$. If $f(t)$ in (28) has a Lipschitz constant C, then the equality $u(t)=\dot{f}(t)$ is satisfied after a finite-time transient process.

Now suppose that the disturbances and uncertainties $\boldsymbol{\eta}$ of the system are Lipschitz continuous. Denote $\boldsymbol{K} = \mathrm{diag}[k_{c1}, k_{c2}]$ with k_{c1} and k_{c2} being positive coefficients, select a sliding surface $\boldsymbol{\sigma}_1 = \widehat{\boldsymbol{e}}_1(t) + \boldsymbol{K}\int_0^t \widehat{\boldsymbol{e}}_1(\tau)\mathrm{d}\tau$, and define a control input as

$$\begin{aligned} &\boldsymbol{u}_2 = -\boldsymbol{G}^{-1}\left(\boldsymbol{f}_2 + \boldsymbol{K}\widehat{\boldsymbol{e}}_1 + \lambda_1|\boldsymbol{\sigma}_1|_*^{1/2}\mathrm{sgn}(\boldsymbol{\sigma}_1) - \boldsymbol{u}_1\right), \\ &\dot{\boldsymbol{u}}_1 = -a_1\mathrm{sgn}(\boldsymbol{\sigma}_1), \end{aligned} \tag{30}$$

where λ_1 and a_1 are the gains, $\mathrm{sgn}(\cdot)$ is the signum function, and $|\boldsymbol{\sigma}_1|_*^{1/2} = \mathrm{diag}\left[|\boldsymbol{\sigma}_1(1)|^{1/2}, |\boldsymbol{\sigma}_1(2)|^{1/2}\right]$.

Theorem 2. Suppose that $v_1 \geqslant V_{1\min} > 0, |\omega_1| < W_{\max}$, $|\theta_e(0)| < \Theta$ for some constants $V_{1\min}$, $W_{\max}$ and Θ, and $\boldsymbol{\eta}$ is with a Lipschitiz constant C. Then, the formation problem can be solved under control law (30), and the orientation error $|\theta_e|$ is bounded if $a_1 > C > 0, \lambda_1 > 0$, and $\Phi(a_1, \lambda_1, C) < 1$.

Proof. The derivative of $\widehat{\boldsymbol{e}}_1$ is $\dot{\widehat{\boldsymbol{e}}}_1 = \boldsymbol{f}_2 + \boldsymbol{G}\boldsymbol{u}_2$, such that the relative degree of the system (27) is $[1, 1]$. The convergence of $\widehat{\boldsymbol{e}}_1$ can be obtained by setting the variable $\dot{\boldsymbol{\sigma}}_1$ to zero. Calculating the derivative of $\boldsymbol{\sigma}_1$, we obtain

$$\dot{\boldsymbol{\sigma}}_1 = \dot{\widehat{\boldsymbol{e}}}_1 + \boldsymbol{K}\widehat{\boldsymbol{e}}_1 = \boldsymbol{f}_2 + \boldsymbol{G}\boldsymbol{u}_2 + K\widehat{\boldsymbol{e}}_1. \tag{31}$$

Considering the uncertainty $\boldsymbol{\eta}$, we can change system (31) into

$$\dot{\boldsymbol{\sigma}}_1 = \boldsymbol{f}_2 + \boldsymbol{\eta} + \boldsymbol{K}\widehat{\boldsymbol{e}}_1 + \boldsymbol{G}\boldsymbol{u}_2. \tag{32}$$

Selecting the control input $\boldsymbol{u}_2$ in (30) and substituting it into (32) give

$$\dot{\boldsymbol{\sigma}}_1 = \boldsymbol{u}_1 - \lambda_1|\boldsymbol{\sigma}_1|_*^{1/2}\mathrm{sgn}(\boldsymbol{\sigma}_1) + \boldsymbol{\eta}, \quad \dot{\boldsymbol{u}}_1 = -a_1\mathrm{sgn}(\boldsymbol{\sigma}_1). \tag{33}$$

Let $\boldsymbol{\eta}_1 = \boldsymbol{u}_1 + \boldsymbol{\eta}$. Then we have

$$\dot{\boldsymbol{\sigma}}_1 = \boldsymbol{\eta}_1 - \lambda_1|\boldsymbol{\sigma}_1|_*^{1/2}\mathrm{sgn}(\boldsymbol{\sigma}_1), \quad \dot{\boldsymbol{\eta}}_1 \in -[a_1 - C, a_1 + C]\mathrm{sgn}(\boldsymbol{\sigma}_1). \tag{34}$$

According to Lemma 2, $\boldsymbol{\sigma}_1$ and $\dot{\boldsymbol{\sigma}}_1$ converge to zero in a finite time. The convergence time is upper bounded by

$$T \leqslant \frac{2}{a_1 - C}\sum_{i=0}^{\infty}|\dot{\boldsymbol{\sigma}}_1(t_i)| = \frac{2|\dot{\boldsymbol{\sigma}}_1(t_0)|}{(a_1 - C)(1 - \Phi(a_1, \lambda_1, C))}, \tag{35}$$

where t_i satisfies $\boldsymbol{\sigma}_1(t_i) = \boldsymbol{0}$.

There are many choices for selecting the gains. For example, we can choose $\lambda_1 = C^{1/2}, a_1 = 1.1C$ ($\Phi = 0.988$) or $\lambda_1 = 0.5C^{1/2}, a_1 = 4C$ ($\Phi = 0.736$). And it is known from (31) that $\widehat{\boldsymbol{e}}_1$ converges to zero exponentially when $\dot{\boldsymbol{\sigma}}_1$ converges to zero.

The proof that θ_e is bounded under control law (30) is similar to that of Theorem 1 and is omitted here.

Remark 1. When there are two or more followers, we could choose one follower as the (virtual) leader of the others. In this way, the leader-follower formation control design method proposed in this paper can be directly applied to the formation control of consequential follower.

5 Examples

In order to validate the theoretical results in this work, we provide two simulation examples. For the adaptive dynamic feedback methodology, we consider two robots moving on a plane: one acts as the leader and the other as the follower. The desired separation distance is $l_{d12} = 1$ m and bearing angle is

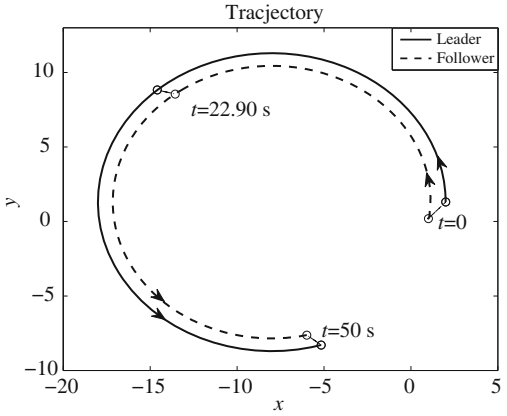

Figure 2 Trajectory of the formation.

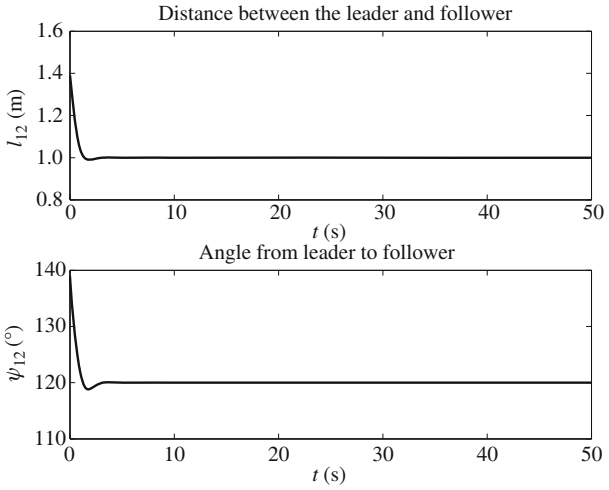

Figure 3 Simulation performance of adaptive dynamic feedback algorithm.

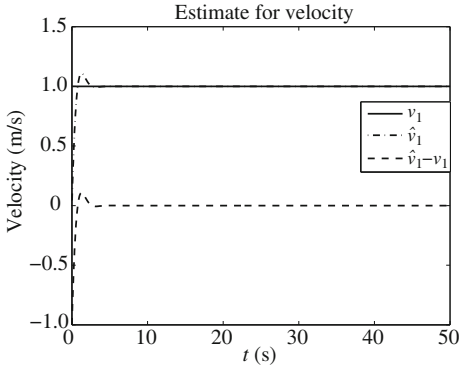

Figure 4 Estimator for the leader robot's linear velocity.

$\psi_{d12} = \frac{2}{3}\pi$ rad. The gains used for the controller presented in the Theorem 1 are $\kappa = 5$ and $k = 3$. Let the initial conditions of the robots be

$$x_1(0) = 2, \quad y_1(0) = 1.3, \quad \theta_1(0) = \frac{1}{2}\pi, \quad x_2(0) = 1, \quad y_2(0) = 0.2, \quad \theta_2(0) = \frac{1}{6}\pi.$$

Suppose that the leader robot moves with a linear velocity $v_1 = 1$ m/s and an angular velocity $\omega_1 = 0.1$ rad/s. The distance between the measured point and the center of the collection of the two rear wheel is $d = 0.1$ m.

Figure 2 shows the trajectory of the formation. It can be seen that the robots form and keep the desired formation after a short transient process. The distance and angle tracking performances are shown in Figure 3. As is evident in Figure 3, the distance and angle approach their desired values quickly. The estimated result for the linear velocity of the leader robot is shown in Figure 4, where $\widehat{v}_1$ stands for the estimated signals. It can be seen that the estimator performs very well.

Next, we proceed with the simulations using the immersion & invariance estimation based second order sliding mode control methodology. The desired separation distance and bearing angle are same as above. And the initial conditions for the two robots are listed below:

$$x_1(0) = 2, \quad y_1(0) = 1.3, \quad \theta_1(0) = \frac{1}{2}\pi, \quad x_2(0) = 1, \quad y_2(0) = 0.2, \quad \theta_2(0) = \frac{1}{6}\pi.$$

The gains in controller (30) are selected as

$$k_{c1} = 5, \quad k_{c2} = 5, \quad a_1 = 0.11, \quad \lambda_1 = 0.474,$$

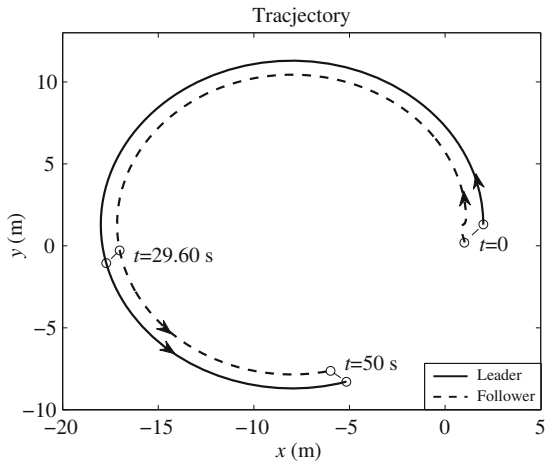

Figure 5 Trajectory of the formation.

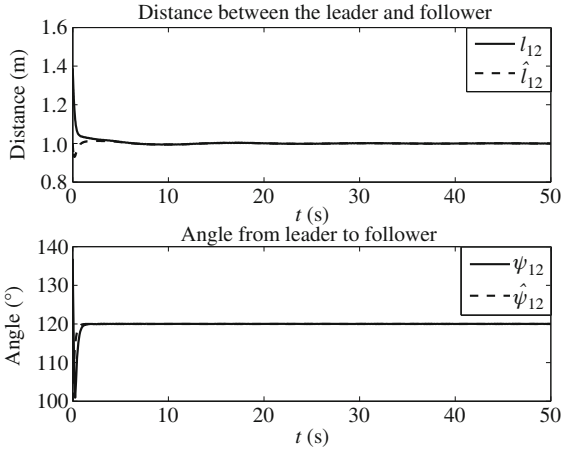

Figure 6 Simulation performance of immersion & invariance based algorithm.

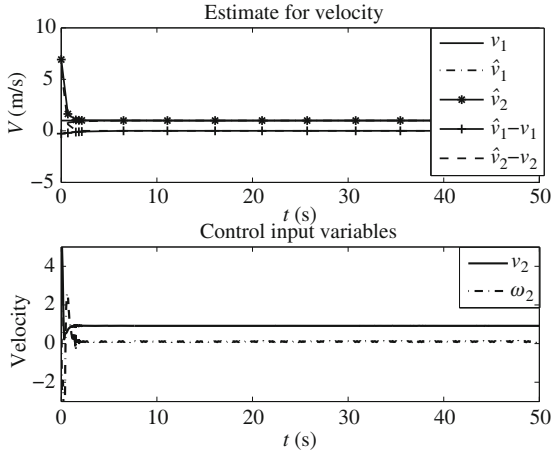

Figure 7 Velocity and control input.

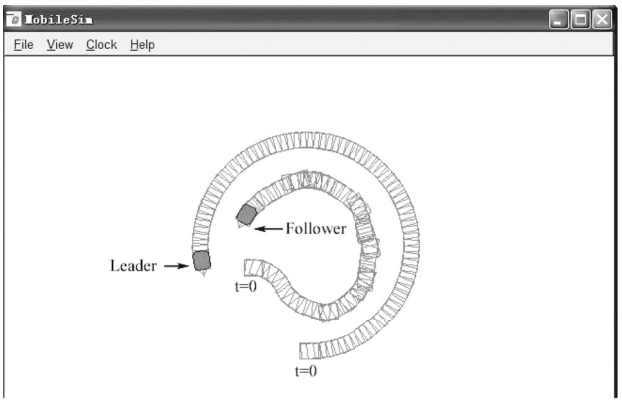

Figure 8 Simulation in MobileSim.

where the parameters in the state and velocity estimators are

$$\lambda_{a1} = 2, \quad \lambda_{a2} = 3, \quad \epsilon = 0.1, \quad \kappa_1 = 3, \quad \kappa_2 = 4, \quad c_1 = 8, \quad c_2 = 10.$$

The uncertainty is assumed as $\boldsymbol{\eta} = [0.01\cos(20t), 0.01\sin(20t)]^{\mathrm{T}}$. Figure 5 shows the trajectory of the controlled formation system. It can be seen that the follower robot tracks the leader robot in a satisfactory manner after a transient time. The tracking variables and their estimates are shown in Figure 6. The leader robot's velocity and its estimate are shown in the upper part of Figure 7. It can be seen that the estimate errors asymptotically converge to zero. The bottom of the Figure 7 illustrates the control inputs of the follower robot.

6 Experiments

The developed control algorithms are implemented on a two AmigoBot robots platform. Both robots are embedded with wireless network devices (WBE2100E) and can communicate with each other. Each of the robots is allocated with an IP address to distinguish from each other. Every robot is installed with two high accuracy encoders on each of the two rear wheels and the relative position l_{12} and ψ_{12} can be calculated from the outputs of the encoders. The control inputs are calculated in a remote host computer and sent to the vehicles through the wireless network. The distance between the center of the two driven wheels to the most front in the axis (the castor) is 0.15 m. First, we focus on the adaptive dynamic feedback algorithm. In this experiment, the leader robot moves with a linear velocity $v_1 = 0.2$

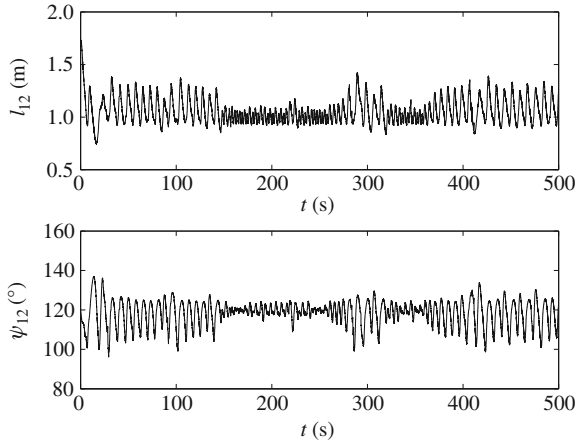

Figure 9 Performance of dynamic feedback algorithm.

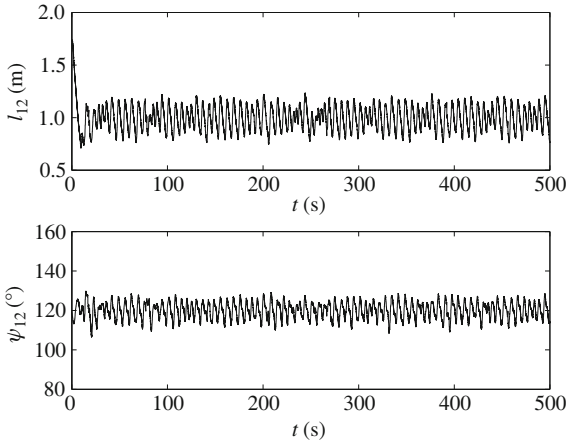

Figure 10 Performance of immersion & invariance based algorithm.

m/s and an angular velocity $\omega_1 = 0.1$ rad/s. The parameters needed for the controllers are chosen as $l_{d12} = 1$ m, $\psi_{d12} = \frac{2}{3}\pi$ rad, $\kappa = 5$, $k = 10$. Figure 8 gives an overview of the tracking performance simulated in MobilesSim®, where the initial positions for the leader robot and follower robot are (0, 0, 0) and (−1, 1.5, 0), respectively. It can be seen that the two robots are not in a desired formation at the beginning. However, under the adaptive dynamic feedback formation controller, the follower robot tracks the leader very well after a transient period. The actual formation performance is shown in Figure 9. These figures show that the adaptive dynamic feedback algorithm works effectively in the robots formation.

Second, we verify the effectiveness of the immersion & invariance estimation based second order sliding mode control algorithm. The initial conditions are set as same as the former experiment and $v_1 = 0.2$ m/s, $\omega_1 = 0.1$ rad/s. The parameters needed for the controllers are chosen as the same as the former simulation section. The experimental performance of the immersion & invariance estimation based second order sliding mode control algorithm running in the robots is presented in Figure 10.

Comparing the simulation results of Figures 2 and 5, and the tracking performances of Figures 3 and 6, we see that the two algorithms have almost the same performance in theory (the two simulations have a same initial condition). Both of the two algorithms can drive the follower robot to track the leader in a short time, and then the tracking parameters approach to their desired values asymptotically. The differences in the performance of the two controllers working in a real physical robot can be obtained by comparing Figure 9 to Figure 10, where the two experiments have a same condition. Generally, the follower robot controlled by both of the two algorithms can form a formation with the leader robot without using the leader robots linear velocity. But the performance in Figure 10 is much better than in Figure 9. Furthermore, the adaptive dynamic feedback algorithm is simpler in deduction and implementation, but largely depending on an accuracy of the model. In contrast, the immersion and invariance based second order sliding mode control algorithm is much more robust at the cost of introducing the auxiliary estimator. The pros and cons of each method offers us a greater flexibility to make decision according to different formation control situations.

7 Conclusion

This paper proposed two control laws for decentralized robots formation control without direct measurement of the leader robot's linear velocity. The adaptive dynamic feedback algorithm utilized the adaptive state feedback method to control the behavior of the follower robot based upon the estimated linear velocity of the leader robot. The immersion & invariance estimation based second order sliding mode control algorithm uses the auxiliary estimators to approximate the leader robot's linear velocity and formation variables, and a second order sliding mode control algorithm was further applied to the augmented sys-

tem. Briefly speaking, the former algorithm is simple in deduction and applications while it is not robust enough. The latter algorithm is much more complex in applications, but it has a better performance of robustness, not only allowing unknown bounded uncertainties but also producing smooth and continuous inputs. The performances of the proposed schemes were verified through numerical examples and physical vehicles experiments.

While the proposed algorithms could deal with the problem without the leader robot's linear velocity, there are some challenging issues in the leader-follower formation control scheme. In our opinion, further research could focus on developing suitable methodologies to meet the requirement of real physical robot systems while enhancing the robot systems' autonomy & intelligence.

Acknowledgements

This work was supported by National Basic Research Program of China (973) (Grant No. 2014CB845302) and National Natural Science Foundation of China (Grant Nos. 61004010, 61273121).

References

1 Dierks T, Jagannathan S. Control of nonholonomic mobile robot formations: backstepping kinematics into dynamics. In: Proceedings of IEEE International Conference on Control Applications, Singapore, 2007. 94–99
2 Dimarogonas D V, Johansson K H. Stability analysis for multi-agent systems using the incidence matrix: quantized communication and formation control. Automatica, 2010, 46: 695–700
3 Zhang F M. Geometric cooperative control of particle formations. IEEE Trans Automat Contr, 2010, 55: 800–804
4 Orqueda O A A, Zhang X T, Fierro R. An output feedback nonlinear decentralized controller for unmanned vehicle co-ordination. Int J Robust Nonlinear Contr, 2007, 17: 1106–1128
5 Desai J P, Ostrowski J, Kumar V. Controlling formations of multiple mobile robots. In: Proceedings of the IEEE Intemational Conference on Robotics and Automation, Leuven, 1998. 2864–2869
6 Das A K, Fierro R, Kumar W, et al. A vision-based formation control framework. IEEE Trans Robot Automat, 2002, 18: 813–825
7 Levant A. Robust exact differentiantion via sliding mode technique. Automatica, 1998, 34: 379–384
8 Levant A. Universal single-input-single output (SISO) sliding-mode controllers with finite-time. IEEE Trans Automat Contr, 2001, 46: 1447–1451
9 Yang J M, Kim J H. Sliding mode control for trajectory tracking of nonholonomic wheeled mobile robots. IEEE Trans Robot Automat, 1999, 15: 578–587
10 Lim H, Kang Y, Kim J, et al. Formation control of leader following unmanned ground vehicles using nonlinear model predictive control. In: Proceedings of the IEEE/ASME International Conference on Advanced Intelligent Mechatronics, Singapore, 2009. 945–950
11 Morbidi F, Mariottini G L, Prattichizzo D. Observer design via immersion and invariance for vision-based leader-follower formation control. Automatica, 2009, 46: 148–154
12 Chowdhary G, Jategaonkar R. Aerodynamic parameter estimation from flight data applying extended and unscented Kalman filter. Aerosp Sci Technol, 2010, 14: 106–117
13 van der Merwe R, Wan E A. The unscented Kalman filter for nonlinear estimation. In: Proceedings of Adaptive Systems for Signal Processing, Communications, and Control Symposium, Lake Louise, Alta, 2000. 153–158
14 Abdessameud A, Tayebi A. On consensus algorithms for double-integrator dynamics without velocity measurements and with input constraints. Syst Contr Lett, 2010, 59: 812–821
15 Krstic M, Kanellakopoulos I, Kokotovic P. Nonlinear and Adaptive Control Design. New York: John Wiley & Sons Inc., 1995
16 Karagiannis D, Astolfi A. Observer design for a class of nonlinear systems using dynamic scaling with appplication to adaptive control. In: Proceedings of the IEEE Conference on Decision and Control, Cancun, 2008. 2314–2319
17 Choi K, Yoo S J, Park J B, et al. Adaptive formation control in absence of leader's velocity information. IET Control Theory Appl, 2010, 4: 521–528